ARTICLE

BIOTECHNOLOGY and BIOENGINEERING

Continuous Modeling of Metabolic Networks With Gene Regulation in Yeast and In Vivo Determination of Rate Parameters

P. Moisset,[1,2] D. Vaisman,[1] A. Cintolesi,[1] J. Urrutia,[1,2] I. Rapaport,[2] B.A. Andrews,[1] J.A. Asenjo[1]

[1]Centre for Biochemical Engineering and Biotechnology, Institute for Cell Dynamics and Biotechnology: A Centre for Systems Biology, University of Chile, Beauchef 850, Santiago, Chile; telephone: 562-978-4283/4723; fax: 562-699-1084; e-mail: juasenjo@ing.uchile.cl

[2]Department of Mathematical Engineering and Centre for Mathematical Modeling, Institute for Cell Dynamics and Biotechnology: A Centre for Systems Biology, University of Chile, Santiago, Chile

ABSTRACT: A continuous model of a metabolic network including gene regulation to simulate metabolic fluxes during batch cultivation of yeast *Saccharomyces cerevisiae* was developed. The metabolic network includes reactions of glycolysis, gluconeogenesis, glycerol and ethanol synthesis and consumption, the tricarboxylic acid cycle, and protein synthesis. Carbon sources considered were glucose and then ethanol synthesized during growth on glucose. The metabolic network has 39 fluxes, which represent the action of 50 enzymes and 64 genes and it is coupled with a gene regulation network which defines enzyme synthesis (activities) and incorporates regulation by glucose (enzyme induction and repression), modeled using ordinary differential equations. The model includes enzyme kinetics, equations that follow both mass-action law and transport as well as inducible, repressible, and constitutive enzymes of metabolism. The model was able to simulate a fermentation of *S. cerevisiae* during the exponential growth phase on glucose and the exponential growth phase on ethanol using only one set of kinetic parameters. All fluxes in the continuous model followed the behavior shown by the metabolic flux analysis (MFA) obtained from experimental results. The differences obtained between the fluxes given by the model and the fluxes determined by the MFA do not exceed 25% in 75% of the cases during exponential growth on glucose, and 20% in 90% of the cases during exponential growth on ethanol. Furthermore, the adjustment of the fermentation profiles of biomass, glucose, and ethanol were 95%, 95%, and 79%, respectively. With these results the simulation was considered successful. A comparison between the simulation of the continuous model and the experimental data of the diauxic yeast fermentation for glucose, biomass, and ethanol, shows an extremely good match using the parameters found. The small discrepancies between the fluxes obtained through MFA and those predicted by the differential equations, as well as the good match between the profiles of glucose, biomass, and ethanol, and our simulation, show that this simple model, that does not rely on complex kinetic expressions, is able to capture the global behavior of the experimental data. Also, the determination of parameters using a straightforward minimization technique using data at only two points in time was sufficient to produce a relatively accurate model. Thus, even with a small amount of experimental data (rates and not concentrations) it was possible to estimate the parameters minimizing a simple objective function. The method proposed allows the obtention of reasonable parameters and concentrations in a system with a much larger number of unknowns than equations. Hence a contribution of this study is to present a convenient way to find in vivo rate parameters to model metabolic and genetic networks under different conditions.

Biotechnol. Bioeng. 2012;109: 2325–2339.

KEYWORDS: continuous modeling of metabolic networks; gene regulation; enzyme synthesis; yeast

Yeast Genome Database: www.yeastgenome.org; Enzyme Database Brenda: www.brenda.uni-koeln.de.

Correspondence to: J.A. Asenjo

Contract grant sponsor: Fondecyt
Contract grant number: 1061119; 1090156
Contract grant sponsor: Millennium Scientific Initiative (ICM)
Contract grant number: P05-001-F
Received: 12 September 2011; Revision received: 13 March 2012;
Accepted: 14 March 2012
Accepted manuscript online 22 March 2012;
Article first published online 24 April 2012 in Wiley Online Library (http://onlinelibrary.wiley.com/doi/10.1002/bit.24503/abstract)
DOI 10.1002/bit.24503

Introduction

Mathematical modeling of biological systems, such as metabolic and genetic networks, is one of the key methodologies of metabolic engineering (Wiechert, 2002). It allows understanding and validation of mechanisms which are involved in metabolism.

Glycolysis, which is considered the heart of basic metabolism, has been widely studied in yeast using mathematical models as well as biochemical approximations (Brusch et al., 2004; Gombert et al., 2001; González et al., 2003; Hynne et al., 2001; Teusink et al., 2000; Wang and Hatzimanikatis, 2006), nevertheless few models include gluconeogenesis (Famili et al., 2003; Rizzi et al., 1997), even though glycolysis and gluconeogenesis are intimately related in the sense that there are some enzymes which are involved in both processes.

During batch growth on glucose *Saccharomyces cerevisiae* presents a respirofermentative first phase where cells grow at their maximum-specific rate; the glucose uptake rate exceeds the capacity for total oxidation and part of it is converted to ethanol and other fermentative products. When glucose is exhausted several genes are activated which allow cells to use ethanol and other products as energy and carbon sources (Daran-Lapujade et al., 2004; Díaz et al., 2009; González et al., 2003; Rolland et al., 2002), and the culture enters the respiratory phase. Moreover, yeast cells use both positive and negative control mechanisms to regulate enzyme levels in order to accomplish this metabolic switch. Enzyme levels are regulated at the stage of gene transcription (repression and induction), mRNA stability, translation, and protein stability (Rolland et al., 2002; Santangelo, 2006).

The purpose of this study is to present a continuous model for simulation and in vivo parameter estimation, in order to represent the behavior of *S. cerevisiae* using glucose and then ethanol as carbon sources using one model and one set of parameters. The model is constructed using enzyme kinetics, the mechanisms of gene expression and enzyme synthesis, as well as data from microarrays. Data from metabolic flux analysis (MFA) is used to fit the equation parameters. Rate parameters are calculated using the Law of Mass Action and Michaelis–Menten kinetics (Bailey and Ollis, 1986).

Methods and Model System

Genetic Network

S. cerevisiae can use different carbon sources according to their availability. The presence of different carbon sources implies that different genes are expressed or repressed. Control of the genetic network can occur at different stages, which can include at least the following: DNA transcription, RNA transport, RNA processing, RNA transduction, and post-translational modifications (Boube et al., 2002; Díaz et al., 2009; Santangelo, 2006). The main mechanisms involved are:

a) Glucose induction (Glycolytic gene expression): Almost all glycolytic steps have genes that are expressed with fermentative and non-fermentative carbon sources. Nevertheless, the presence of glucose triggers the induction of the expression of most glycolytic genes and some glucose transporters, especially in the lower part of the glycolysis and fermentation pathway (Benanti et al., 2007; Müller et al., 1995; Özcan et al., 1996; Zhang et al., 2009). The increase of this glycolytic capacity is essential for efficient energy generation (Rolland et al., 2002; Santangelo, 2006). The main gene families induced by glucose considered were *hxt*, *glk*, *pfk*, *pdc*, *adh*, *pda*, *pdb*, *lpd*, *pdx*, and *pyc*.
b) Glucose repression (Gluconeogenic gene expression): This pathway is responsible for the downregulation of respiration, gluconeogenesis, and the transport and catabolic capacity of alternative sugars during growth on glucose (Gancedo, 1998; Özcan et al., 1998; Rolland et al., 2002; Schüller, 2003). The main gene families repressed by glucose considered were *fbp*, *adh2*, *ald2*, *acs*, *pck1*, *cit2*, and *idp*.

In order to complete the information of the regulatory genetic network in *S. cerevisiae*, information from the study on gene expression in yeast of Díaz et al. (2009) was used.

Metabolic Network

The reaction network was constructed to include glycolysis, gluconeogenesis, tricarboxylic acid (TCA) cycle, and fermentation reactions. Main protein production pathways were taken into consideration according to the metabolic network presented by González et al. (2003). The pentose phosphate pathway (PPP) was not included since González et al. (2003) showed that it represented relatively small fluxes compared to the others considered in the network. Figure 1 shows the network used in the present study.

Interaction Between Metabolic Network and Regulatory Genetic Network

The genetic regulatory network interacts with the metabolic network (Cox et al., 2005; Gagneur and Casari, 2005) since the expression of genes, synthesizing enzymes, determines the terminal velocities of the fluxes of the metabolic routes. On the other hand, the concentration of the internal metabolites of the metabolic network can regulate gene expression, thus influencing the regulatory genetic network. Asenjo et al. (2007) investigated a discrete mathematical model of gene regulation of metabolism in *Escherichia coli* using three different carbon sources. Figure 2 shows the interactions that take place including glucose induction and glucose repression.

Rate Equations of the System and Enzyme Synthesis

Hynne et al. (2001) proposed a method to compute some kinetic constants when the expression for the dynamics are

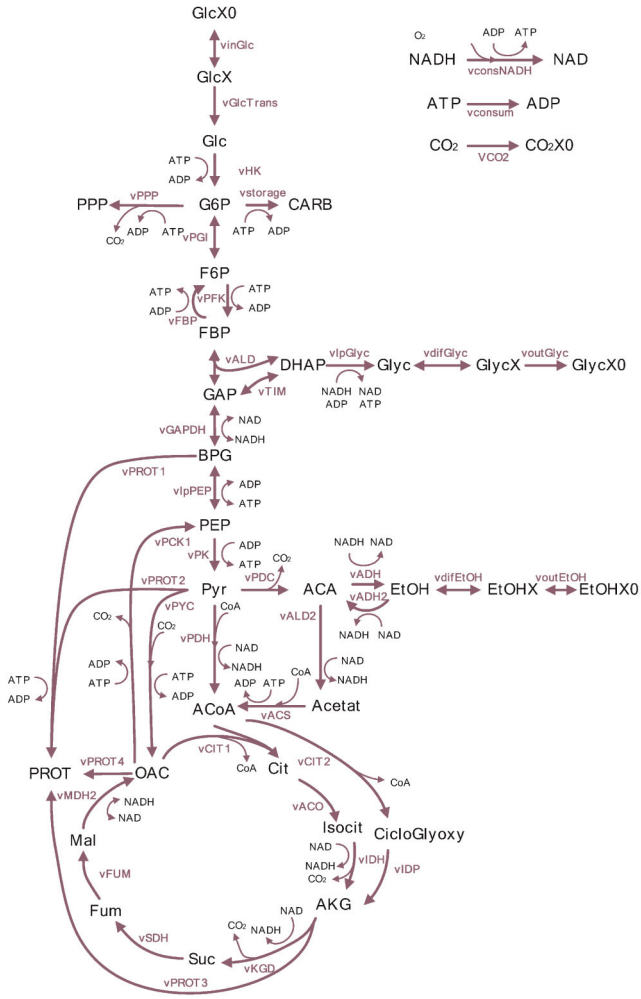

Figure 1. Reaction network of the model. [Color figure can be seen in the online version of this article, available at wileyonlinelibrary.com]

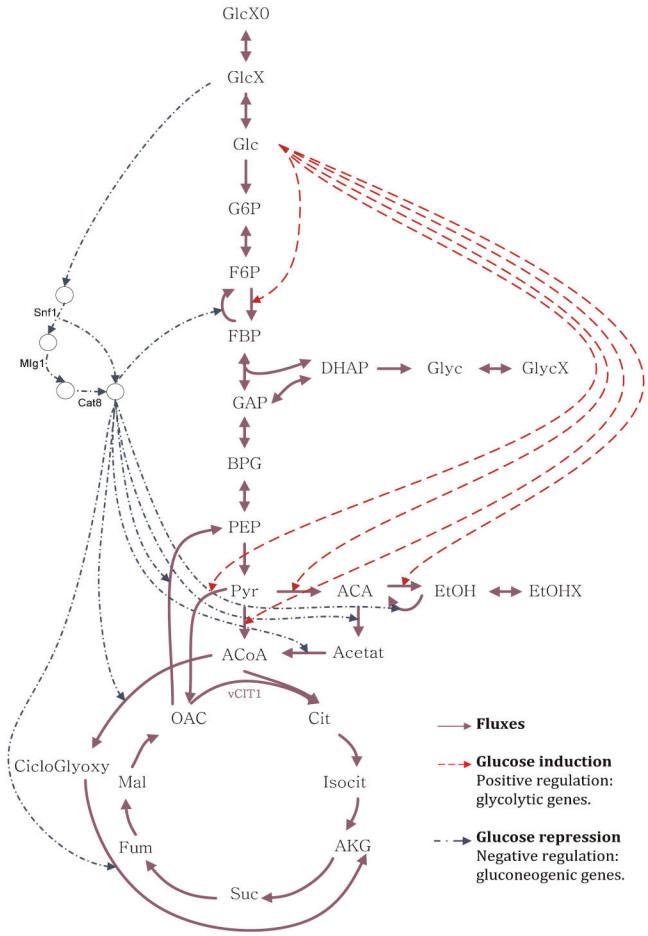

Figure 2. Interactions between metabolic network and regulatory genetic network. Continuous lines represent reactions in the metabolic network; Broken lines represent transcription factors or enzymes; Nodes represent transcription factors in the genetic network. Different colors represent different genetic regulation mechanisms. Blue: glucose repression (Negative regulation. Gluconeogenic genes); Red: glucose induction (Positive regulation. Glycolytic genes). [Color figure can be seen in the online version of this article, available at wileyonlinelibrary.com]

rational functions. Hynne's method assumes that the metabolite concentrations in the cell are known or can be reasonably estimated. They also assumed that the constants in the denominator of the rational expressions are known. When all this information is available, the determination of the kinetic constants appearing in the numerator reduces to a linear algebra problem. However, this is not usually the case since not all the data are fully available in the literature. Many kinetic constants have been computed for in vitro conditions and not in vivo and measured concentrations of metabolites vary from one publication to another even if the experimental conditions are relatively similar (Albe et al., 1990; Lagunas and Gancedo, 1983; Theobald et al., 1997).

To overcome some of these difficulties, simplified reaction dynamics were used based in most cases on mass-action kinetics. Given the limited quantity and quality of experimental data, parts of the problem of reverse engineering kinetic constants and concentrations is underdetermined, while others are over-determined. To work around these problems, reasonable regularization conditions were imposed and then the resulting non-linear problem was solved using a standard iterative numerical algorithm.

In the case of the enzymatic reactions, it was considered that the rate equations correspond to kinetics of the Michaelis–Menten type. As virtually all reaction substrates in the cell are at relatively low concentrations (Albe et al., 1990; Lagunas and Gancedo, 1983; Theobald et al., 1997) it can be safely assumed that the enzyme catalyzed reactions are of first order with respect to the substrate. This is an important simplification given the fact that metabolite concentrations in the cell are relatively low, and in most cases lower or similar than the values of K_m. For instance in Equations (8 and 9), the Michaelis constants (K_m) found by previous authors are 1.23 and 4.0 mM, respectively (0.21 and

0.68 g/L; Hynne et al., 2001 and Rizzi et al., 1997), which are similar or even higher than the concentrations of metabolites of 0.24 and 0.12 g/L on glucose and on ethanol for DHAP in our work (Eq. 8), and of 0.26 and 0.13 g/L on glucose and ethanol for GAP (Eq. 9). For the purposes of this study, where the aim is to carry out simulations at steady-state, with constant metabolite concentrations but at different conditions, the further complexity of complete Michaelis–Menten kinetics does not appear necessary. This will be confirmed with the quality of the results obtained. Hence, the enzyme kinetics correspond to an irreversible reaction with a single substrate as shown in the following equation:

$$v = k[E][S] \tag{1}$$

where v is the rate of the enzymatic reaction, $[E]$ is the enzyme concentration, and $[S]$ the substrate concentration. This last expression can be rewritten considering a normalized enzymatic factor, e, in the following way:

$$v = k' \frac{[E]}{[E]_{\max}}[S] \tag{2}$$

$$v = ek'[S] \tag{3}$$

where $e = \frac{[E]}{[E]_{\max}}$

For constitutive enzymatic reactions it will be considered that $e = 1$.

The Method in Detail

The continuous model is a system of ordinary differential equations that follow a standard form

$$\frac{dC}{dt} = S \times v \tag{4}$$

where S is the stoichiometric matrix and v is a vector of velocities. Mass-action kinetics were assumed for the internal non-enzymatic reactions of the cell and simplified Michaelis–Menten kinetics (first order) for the internal enzymatic reactions. Most of the enzymatic reactions have constitutive enzyme expression. These rate equations of the model are presented in Table I. All equations that include the parameter e_1 correspond to enzymes that are glucose-induced and those that include e_2 are glucose repressed. The rest are either constitutive enzymes or transport equations or mass-action law type. These expressions are augmented with some extra equations to model biomass production and ethanol, glucose, and glycerol transport to/from the cell membrane from/to the extracellular medium. There are also equations to model gene expression by mRNA and enzyme synthesis. These equations will be described later.

The genes and enzymes that participate in each reaction are shown in Appendix 1. To simplify the model, every reaction has been considered to be dependent on one enzyme synthesized by one molecule of mRNA. This is a normal simplification as usually one enzyme in a particular reaction of the metabolism can be considered to be the one that controls the specific reaction. This would be a normal assumption for a simplified model such as ours and should not affect the model outcome.

To define the values of enzyme expression, information of the regulatory genetic network has been considered. Most of the gluconeogenic genes are repressed by the presence of glucose, which means that the enzymes are not being synthesized during this phase and that they are expressed when glucose is depleted. A number of glycolytic and fermentative enzymes behave in exactly the opposite way, being induced by the presence of glucose (Benanti et al., 2007; Gancedo, 1998; Müller et al., 1995; Özcan et al., 1996, 1998; Rolland et al., 2002; Schüller, 2003). The rest are considered to have a constitutive expression. This process was modeled considering the mRNA synthesis rate regulated by glucose and the enzyme synthesis rate, based partially on previous models (Alon, 2007; Bailey and Ollis, 1986; Hatzimanikatis, 2010; Jacob and Monod, 1961; Kaushik et al., 1979; Yagil and Yagil, 1971).

Each enzyme expression rate is determined by its mRNA concentration and its degradation rate, as follows:

$$\frac{d[E]}{dt} = K_{enz1}[\text{mRNA}] - K_{enz2}[E] \tag{5}$$

For the purposes of our model, we only need to model the e enzymatic factor. The value of e must go from 0 (no expression) to 1 (maximum expression).

The transition of the e factors between 0 and 1 is very fast compared to the time of the complete simulation. Therefore, a simple model like a Hill function, suffices. The simplified model for enzyme synthesis is:

For induction:

$$\frac{d([\text{mRNA}_1])}{dt} = K_{\text{mRNA}}\left(\frac{[\text{Glc}]^{\alpha}}{0.05^{\alpha} + [\text{Glc}]^{\alpha}} - [\text{mRNA}_1]\right) \tag{6}$$

$$\frac{d[e_1]}{dt} = K_{enz}([\text{mRNA}_1] - [e_1]) \tag{7}$$

For repression:

$$\frac{d([\text{mRNA}_2])}{dt} = K_{\text{mRNA}}\left(\frac{0.05^{\alpha}}{0.05^{\alpha} + [\text{Glc}]^{\alpha}} - [\text{mRNA}_2]\right) \tag{8}$$

$$\frac{d[e_2]}{dt} = K_{enz}([\text{mRNA}_2] - [e_2]) \tag{9}$$

The value 0.05 [mmol/g cell] is the threshold of glucose concentration at which the transition occurs. Hence, when $[\text{Glc}] < 0.05$ [mmol/g cell] it can be considered that there is no more glucose available. The values for K_{mRNA} and K_{enz} are chosen so the mean degradation times for mRNA and

Table I. Rate equations.

1	V_{inGlc}	$\text{Glc}_{x0} \leftrightarrow \text{Glc}_x$ $K_{\text{vinGlc}}\left(\frac{[\text{Glc}_{x0}]}{K_{\text{conv}}} - [\text{Glc}_x]\right)$
2	V_{GlcTrans}	$\text{Glc}_x \rightarrow \text{Glc}$ $\frac{K_{\text{VGlc1}}[\text{Glc}_x]}{K_{\text{VGlc2}}+[\text{Glc}_x]}$
3	V_{HK}	$\text{Glc} + \text{ATP} \rightarrow \text{G6P} + \text{ADP}$ $e_1 K_{\text{vHK}}[\text{Glc}][\text{ATP}]$
4	V_{PGI}	$\text{G6P} \leftrightarrow \text{F6P}$ $K_{\text{vPGI,f}}[\text{G6P}] - K_{\text{vPGI,r}}[\text{F6P}]$
5	V_{PFK}	$\text{F6P} + \text{ATP} \rightarrow \text{FBP} + \text{ADP}$ $e_1 K_{\text{vPFK}}[\text{F6P}][\text{ATP}]$
6	V_{FBP}	$\text{FBP} + \text{ADP} \rightarrow \text{F6P} + \text{ATP}$ $e_2 K_{\text{vFBP}}[\text{FBP}][\text{ADP}]$
7	V_{ALD}	$\text{FBP} \leftrightarrow \text{GAP} + \text{DHAP}$ $K_{\text{vALD,f}}[\text{FBP}] - K_{\text{vALD,r}}[\text{DHAP}]$
8	V_{TIM}	$\text{DHAP} \leftrightarrow \text{GAP}$ $K_{\text{vTIM,f}}[\text{DHAP}] - K_{\text{vTIM,r}}[\text{GAP}]$
9	V_{GAPDH}	$\text{GAP} + \text{NAD} \leftrightarrow \text{BPG} + \text{NADH}$ $K_{\text{vGAPDH,f}}[\text{GAP}][\text{NAD}] - K_{\text{vGAPDH,r}}[\text{BPG}][\text{NADH}]$
10	V_{IpPEP}	$\text{BPG} + \text{ADP} \leftrightarrow \text{PEP} + \text{ATP}$ $K_{\text{vlpPEP,f}}[\text{BPG}][\text{ADP}] - K_{\text{vlpPEP,r}}[\text{PEP}][\text{ATP}]$
11	V_{PK}	$\text{PEP} + \text{ADP} \rightarrow \text{Pyr} + \text{ATP}$ $K_{\text{vPK}}[\text{PEP}][\text{ADP}]$
12	V_{PDC}	$\text{Pyr} \rightarrow \text{ACA} + \text{CO}_2$ $e_1 K_{\text{vPDC}}[\text{Pyr}]$
13	V_{ADH}	$\text{ACA} + 2\text{NADH} \rightarrow \text{EtOH} + 2\text{NAD}$ $e_1 K_{\text{vADH}}[\text{ACA}][\text{NADH}]^2$
14	V_{ADH2}	$\text{EtOH} + 2\text{NAD} \rightarrow \text{ACA} + 2\text{NADH}$ $e_2 K_{\text{vADH2}}[\text{EtOH}][\text{NAD}]^2$
15	V_{difEtoH}	$\text{EtOH} \leftrightarrow \text{EtOH}_x$ $K_{\text{vdifEtOH,f}}[\text{EtOH}] - K_{\text{vdifEtOH,r}}[\text{EtOH}_x]$
16	V_{outEtoH}	$\text{EtOH}_x \leftrightarrow \text{EtOH}_{x0}$ $K_{\text{voutEtOH}}\left([\text{EtOH}_x] - \frac{[\text{EtOH}_{x0}]}{K_{\text{conv}}}\right)$
17	V_{IpGlyc}	$\text{DHAP} + \text{NADH} + \text{ADP} \rightarrow \text{Glyc} + \text{NAD} + \text{ATP}$ $K_{\text{vlpDlyc}}[\text{DHAP}]$
18	V_{difFlyc}	$\text{Glyc} \leftrightarrow \text{Glyc}_x$ $K_{\text{vdifGlyc}}([\text{Glyc}] - [\text{Glyc}_x])$
19	V_{outGlyc}	$\text{Glyc}_x \rightarrow \text{Glyc}_{x0}$ $K_{\text{voutGlyc}}[\text{Glyc}_x]$
20	V_{storage}	$\text{G6P} + \text{ATP} \rightarrow \text{CARB} + \text{ADP}$ $K_{\text{vstorage}}[\text{ATP}][\text{G6P}]$
21	V_{ALD2}	$\text{ACA} + \text{NAD} \rightarrow \text{Acetat} + \text{NADH}$ $e_2 K_{\text{vALD2}}[\text{ACA}][\text{NAD}]$
22	V_{ACS}	$\text{Acetat} + 2\text{ATP} + \text{CoA} \rightarrow \text{ACoA} + 2\text{ADP}$ $e_2 K_{\text{vACS}}[\text{Acetat}][\text{ATP}]^2[\text{CoA}]$
23	V_{PDH}	$\text{Pyr} + \text{NAD} + \text{CoA} \rightarrow \text{ACoA} + \text{NADH} + \text{CO}_2$ $e_1 K_{\text{vPDH}}[\text{Pyr}][\text{NAD}][\text{CoA}]$
24	V_{PYC}	$\text{Pyr} + \text{ATP} + \text{CO}_2 \rightarrow \text{OAC} + \text{ADP}$ $e_1 K_{\text{vPYC}}[\text{Pyr}][\text{ATP}]$
25	V_{CIT1}	$\text{AcoA} + \text{OAC} \rightarrow \text{Cit} + \text{CoA}$ $K_{\text{vCIT1}}[\text{ACoA}][\text{OAC}]$
26	V_{ACO}	$\text{Cit} \rightarrow \text{Isocit}$ $K_{\text{vACO}}[\text{Cit}]$
27	V_{IDH}	$\text{Isocit} + \text{NAD} \rightarrow \text{AKG} + \text{NADH} + \text{CO}_2$ $K_{\text{vIDH}}[\text{Isocit}][\text{NAD}]$
28	V_{KGD}	$\text{AKG} + \text{NAD} \rightarrow \text{Suc} + \text{NADH} + \text{CO}_2$ $K_{\text{vKGD}}[\text{AKG}][\text{NAD}]$
29	V_{SDH}	$\text{Suc} \rightarrow \text{Fum}$ $K_{\text{vSDH}}[\text{Suc}]$
30	V_{FUM}	$\text{Fum} \rightarrow \text{Mal}$ $K_{\text{vFUM}}[\text{Fum}]$
31	V_{MDG2}	$\text{Mal} + \text{NAD} \rightarrow \text{OAC} + \text{NADH}$ $K_{\text{vMDDH2}}[\text{Mal}][\text{NAD}]$

(*Continued*)

Table I. (*Continued*)

32	V_{PCK1}	$OAC + ATP \rightarrow PEP + ADP + CO_2$ $e_2 K_{vPCK1}[OAC][ATP]$
33	V_{CIT2}	$ACoA \rightarrow CicloGlyoxy + CoA$ $e_2 k_{vCIT2}[ACoA]$
34	V_{IDP}	$CicloGlyoxy \rightarrow AKG$ $e_2 K_{vIDP}[CicloGlyoxy]$
35	V_{PROT}	$0.1246\,Pyr + 0.10830\,AC + 0.138\,BPG + 0.1553\,AKG + 4.3\,ATP \rightarrow PROT + 4.3\,ADP$ $K_{PROT1}[BPG][ATP] + K_{PROT2}[PYR][ATP] + K_{PROT3}[AKG][ATP] + K_{PROT4}[OAC][ATP]$
36	V_{PPP}	$G6P + ATP \rightarrow PPP + ADP + CO_2$ $K_{vPPP}[G6P][ATP]$
37	$V_{consNADH}$	$2\,NADH + 2.48\,ADP + O_2 \rightarrow 2\,NAD + 2.48\,ATP$ $K_{vconsNADH}[NADH]^2[ADP]^2$
38	V_{consum}	$ATP \rightarrow ADP$ $K_{vconsum}[ATP]$
39	V_{CO2}	$CO_2 \leftrightarrow CO_{2x0}$ $K_{vCO2}([CO_2] - [CO_{2x0}])$

the enzymes are in the order of minutes. The values for K_{mRNA} and K_{enz} and α used are shown in Table II.

Most equations in the model follow the $(dC/dt) = S \times v$ formulation, where v is obtained using the Law of Mass Action. However, some do not, and enzyme synthesis is one of those exceptions. The other exceptions are the equations that account for glucose and ethanol transport between the medium and the cell membrane. The glucose equation is:

$$\frac{dGlcX0}{dt} = -K_{vinGlc}\left(\frac{GlcX0}{K_{conv}} - GlcX\right)Biomass \qquad (10)$$

K_{conv} serves two purposes, it captures the equilibrium constant of the transport process and also does a conversion of units. This conversion is needed because GlcX0 is in g/L, while GlcX is in mmol/g cell. The equation that describes ethanol transport between the cell membrane and the growth medium and vice versa is:

$$\frac{dEtOHX0}{dt} = K_{voutEtOH}\left(EtOHX - \frac{EtOHX0}{K_{conv}}\right)Biomass^{1.9} \qquad (11)$$

The experimental data (González et al., 2003) shows that ethanol consumption is proportional to biomass to a power of ca. 1.9–2.0. The biomass equation is:

$$\frac{dBiomass}{dt} = K_{yield} \times vPROT \times Biomass \qquad (12)$$

Table II. Values of constants used in the expressions for enzyme induction and repression and for biomass growing on glucose and ethanol.

K_{mRNA}	25.0
K_{enz}	12.5
α	10.0
K^g_{yield}	0.317
K^e_{yield}	0.173

where $K_{yield} = K^g_{yield}$ on glucose and $K_{yield} = K^e_{yield}$ on ethanol. The values of these parameters are also shown in Table II.

We assumed that the rate of biomass production is proportional to the protein production rate. The experimental data (González et al., 2003) shows that the yield constant is different when the cells are growing on glucose or on ethanol.

Finally, vGlcTrans is the rate at which glucose is transferred from the cell membrane to the cytoplasm:

$$vGlcTrans = \frac{5[mmol/g\,cell\,h] \times GlcX}{0.05[mmol/g\,cell] + GlcX} \qquad (13)$$

In González's work (2003) it is seen that this rate is roughly 5 [mmol/g cell] regardless of the amount of glucose available. The rate, of course, must drop to zero when all the glucose in the growth media has been depleted. The function we use for vGlcTrans gives a constant value when $[GlcX] \gg 0.005$ [mmol/g cell].

By analyzing the left kernel of the stoichiometric matrix s, we determine that our differential equations preserve three quantities: ATP + ADP, NAD + NADH, and ACoA + CoA. This is important for the determination of all the model's parameters.

Results and Discussion

As a result of this work a metabolic network with 39 fluxes that include glycolysis, TCA cycle, and gluconeogenesis, as well as fluxes towards the routes of protein production and the PPP was continuously modeled, including gene regulation of enzyme synthesis. These fluxes represent the interaction of 50 enzymes and 64 genes.

Metabolic Flux Analysis (MFA) Phase

The first step is to determine the internal network fluxes from some measured external fluxes. All the measured fluxes

used in this study were from González et al. (2003) taken from the raw data when cells are in steady-state, growing exponentially on glucose, and then exponentially on ethanol at a constant-specific growth rate. Hence in a small Δt (period of time) a pseudo stationary state of the network can be assumed. The MFA problem was resolved using the metabolic network proposed in this study, at two points in time, one during the exponential growth on glucose phase and the other during the exponential growth on ethanol. These vectors of fluxes will be called f_g and f_e, and the times at which the fluxes were sampled will be denoted as t_g and t_e, respectively. The results of the fluxes of the simplified model of MFA are shown in Figure 3.

Determination of Kinetic Parameters and Metabolite Concentrations

After computing f_g and f_e, a vector of kinetic constants K and vectors of concentrations C_g and C_e, were determined such that

$$V(K, C_g) = f_g$$
$$V(K, C_e) = f_e$$

where V is the vector of kinetic expressions, and C_g and C_e are vectors of concentrations at t_g and t_e. The kinetic expressions are shown in Table II. There are a total of 72 equations and 120 unknowns in this system. In the cases where reactions are defined as reversible, the ratio of both constants is equal to the equilibrium constant of the reaction. In general, this set of equations may not have a solution, especially when the vectors f_g and f_e contain some error. Since f_g and f_e were computed from experimental data they should be considered estimated quantities. The standard technique to handle indetermination is minimizing some form of error expression, sometimes called a residue. The number of unknowns is much larger than the number of equations, thus we expect some constants and/or concentrations to be underdetermined. Ideally, one could use measurements of concentrations of all metabolites in the cell to reduce the number of degrees of freedom. This would also have the advantage of turning our non-linear system of equations into a linear one. Unfortunately, a number of metabolite concentrations are not available in the literature and/or they vary more than one order of magnitude in some cases even if experimental conditions are relatively similar (Albe et al., 1990; Lagunas and Gancedo, 1983; Theobald et al., 1997). One approach to find a solution is to impose some regularization conditions that favor answers with desirable properties. In our case, we would like concentrations and constants not to be "too large" as they would be physically unrealistic conditions for a biological system. Also, the kinetic constants cannot be "too small," as this would considerably slow down the convergence rate to equilibrium. A final constraint we have to enforce is the preservation of some quantities. In our model, for example, ATP + ADP is preserved, therefore, $C_{g,ATP} + C_{g,ADP} = C_{e,ATP} + C_{e,ATP}$.

Such a procedure, described in detail below, can be used for regularization of inverse problems such as the present one, particularly when there are more unknowns than equations (Engl et al., 2000).

The final expression for the residue we wish to minimize is

$$R = \alpha_w^2 \sum_i \left(\frac{K_{i,f} \times r_{i,f} - K_{i,b} \times r_{i,b}}{f_{MFA,i}} - 1 \right)^2 + \text{a priori} + \gamma_w^2 \sum_k C_k^2 + \delta_w^2 \sum_l (K_l - 5)^2 + \text{conservation} \quad (14)$$

where

$$\text{a priori} = \varphi_w^2 \left[\left(C_{GlcX0,g} - \hat{C}_{GlcX0,g} \right)^2 + \left(C_{GlcX,g} - \frac{\hat{C}_{GlcX0,g}}{k_{conv}} \times 0.995 \right)^2 \right] + \left(C_{EtOHX0,e} - \hat{C}_{EtOHX0,e} \right)^2 + \beta_w^2 \left(C_{GlcX0,e}^2 + C_{GlcX,e}^2 \right) \quad (15)$$

$$\text{conservation} = \varepsilon_w^2 \left[\left(C_{ATP,g} + C_{ADP,g} - C_{ATP,e} - C_{ADP,e} \right)^2 + \left(C_{NAD,g} + C_{NADH,g} - C_{NAD,e} - C_{NADH,e} \right)^2 + \left(C_{CoA,g} + C_{ACoA,g} - C_{CoA,e} - C_{ACoA,e} \right)^2 \right] \quad (16)$$

The terms of R associated with α_w are intended to minimize the relative error of the fluxes predicted by the continuous model. More precisely, the ratio between the ith flux at equilibrium of the ODE system $(K_{i,f} \times r_{i,f} - K_{i,b} \times r_{i,b})$ and the value obtained by the MFA $(f_{MFA,i})$ should be close to one. Similarly, we added terms corresponding to the regularization conditions. The a priori term is intended to make the concentrations predicted by the model similar to those given by our somewhat simplified model for the MFA shown in Figure 3, which is based on the experimental data of González et al. (2003). The terms $\hat{C}_{GlcX0,g}$, $\hat{C}_{GlcX0,g}$, and $\hat{C}_{EtOHX0,e}$ are measured quantities, while the variables without the hat are variables of the ODE. The last terms correspond to the preservation of quantities. The 0.995 factor used in R was a simple mathematical consideration to force $C_{GlcX,g}$ to be slightly lower than $\hat{C}_{GlcX0,g}/K_{conv}$, which indirectly forces K_{vinGlc} to have a large value. The terms multiplied by γ_w^2 and δ_w^2 avoid concentrations being too large, while making it undesirable for a rate

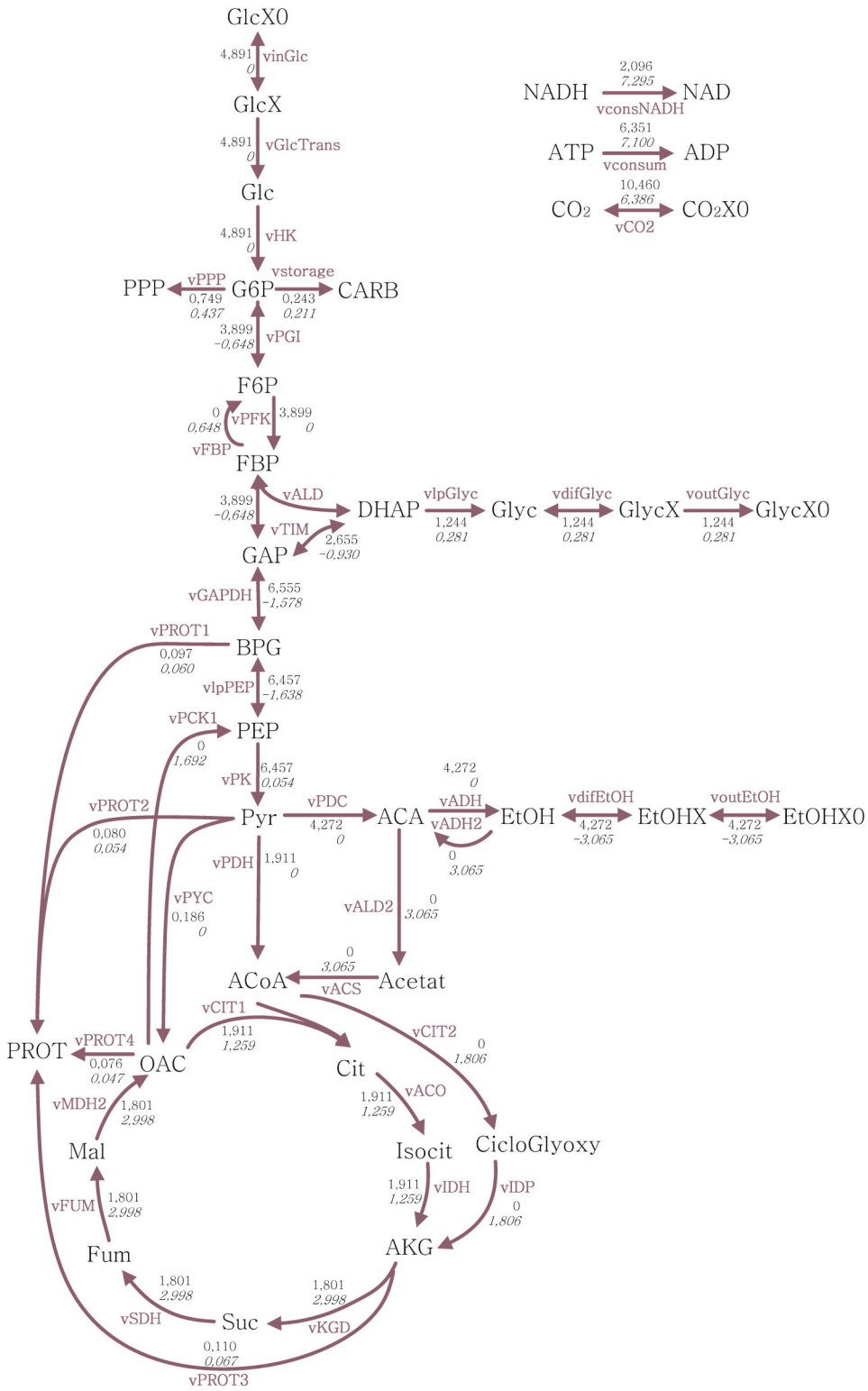

Figure 3. Distribution of metabolic fluxes at different growth phases: (1) exponential growth on glucose (top values) and (2) exponential growth on ethanol (bottom values in italics). Flux values are expressed in mmol/g cell h. [Color figure can be seen in the online version of this article, available at wileyonlinelibrary.com]

parameter to be far away from 5. Too small a rate parameter increases the time the system needs to reach equilibrium. Our choice of 5 as a desired valued is somewhat arbitrary, but based on the timescale of the problem at hand. In any case, the value we used for δ_w is very small, so this constraint does not play an important role unless a rate constant is completely undetermined. The terms that define the *conservation* simply state that the preserved quantities must be the same at t_g and t_e.

The coefficients α_w, β_w, γ_w, δ_w, ε_w, and φ_w are the weights of each constraint. The exact values used for weights are not critical as long as their relative magnitudes represent how important it is to satisfy each constraint. For example, since we know for sure that some quantities are preserved, we assigned a large value to ε_w. For practical purposes, this acts as a "hard" constraint, enforcing equality. For the regularization conditions we imposed for concentrations and kinetic rates, we used much smaller coefficients (γ_w and δ_w), making those constraints fairly weak. Table III shows the values of the weight coefficients that were used.

R was minimized using Matlab's function lsqnlin. The objective function has multiple local minima. This was handled by running the optimizer 100 times starting from a randomly chosen point. The chosen solution corresponds to the smallest residue found. The kinetic constants found, which are shown in Table IV, are the result of this optimization. Another result of the optimization were the vectors C_g and C_e, which are estimations of the equilibrium points of the system when growing on glucose and ethanol, respectively.

Concerning the parameters used for the enzymatic reactions, the constants α, K_{mRNA}, and K_{enz} are used to model the presence or absence of certain enzymes. The values used for K_{mRNA} and K_{enz} were calculated so the half degradation times for the mRNA and the enzymes is about 2 min.

The yield coefficients were calculated based on the experimental results of González (2003), where the maximum-specific growth rate during the glucose phase was $\mu_{max} = 0.159$ [1/h], and the maximum-specific growth rate during the ethanol phase was $\mu_{max} = 0.070$ [1/h], which are both constants. From Equation (12).

$$\frac{\text{dBiomass}}{\text{d}t} = K_{\text{yield}} \times \text{vPROT} \times \text{Biomass}$$

it is easy to estimate values for K^g_{yield} and K^e_{yield} because the values of vPROT and Biomass at t_g and t_e, are known during exponential growth

$$\frac{\text{dBiomass}}{\text{d}t} = \mu_{max} \times \text{Biomass} \tag{17}$$

Therefore,

$$K_{\text{yield}} = \frac{\mu_{max}}{\text{vPROT}} \tag{18}$$

The calculated values of K^g_{yield} and K^e_{yield} are 0.408 and 0.163 respectively. Both K^g_{yield} and K^e_{yield} (Table II) were

Table III. Weight coefficients and their values.

Weight coefficient	Value
α_w	1.0
β_w	0.1
γ_w	0.01
δ_w	0.0001
ε_w	150
φ_w	10,000

Table IV. Kinetic constants of the model.

K_{vinGlc}	363
K_{conv}	32.0
K_{vGlc1}	5.00
K_{vGlc2}	0.05
K_{vHK}	33.2
$K_{vPGI,f}$	1470
$K_{vPGI,r}$	264
K_{vPFK}	20.7
K_{vFBP}	6.47
$K_{ALD,f}$	356
$K_{vALD,r}$	471
$K_{vTIM,f}$	841
$K_{vTim,r}$	773
$K_{vGAPDH,f}$	59.1
$K_{vGAPDH,r}$	618
$K_{vlpPEP,f}$	825
$K_{vlpPEP,r}$	168
K_{vPK}	1.73
K_{vPDC}	279
K_{vADH}	33.3
K_{vADH2}	41.4
$K_{vdifEtoH,f}$	542
$K_{vdifEtoH,r}$	309
$K_{voutEtoH,f}$	8.05
$K_{vlpGlyc}$	2.76
$K_{vdifGlyc}$	14.6
$K_{voutGlyc}$	18.0
$K_{vstorage}$	7.50
K_{vALD2}	26.0
K_{vACS}	74.6
K_{vPDH}	142
K_{vPYC}	23.5
K_{vCIT1}	97.8
K_{vACO}	17.1
K_{vIDH}	31.1
K_{vKGD}	232
K_{vSDH}	24.7
K_{vFUM}	24.0
K_{vMDH2}	25.1
K_{vPCK1}	106
K_{vCIT2}	3.59
K_{vIDP}	16.9
K_{vPROT1}	1.03
K_{vPROT2}	9.81
K_{vPROT3}	12.4
K_{vPROT4}	9.36
K_{vPPP}	18.9
$K_{vconsNADH}$	9.34
$K_{vconsum}$	11.9
K_{vCO2}	51.2

adjusted so that the model adequately fitted the experimental data over the whole period of both exponential phases on glucose and on ethanol.

Model Validation

After the determination of the model parameters, we integrated the model and compared its output against the experimental results obtained by MFA (Fig. 3). Simulation of the ordinary differential equations was done using MatLab's ode23tb function because of the ODEs exhibiting stiffness. The initial concentrations were the values of the C_g vector obtained by the residue minimization process described above. As mentioned before a number of metabolite concentrations are not available or vary more than one order of magnitude in the published literature (Albe et al., 1990; Lagunas and Gancedo, 1983; Theobald et al., 1997). However, those obtained in the simulations carried out using our model are very similar to those obtained by Albe et al. (1990) and Theobald et al. (1997). For instance, in our simulations we obtained ATP concentrations of 0.52 g/L in the glucose phase and 0.61 g/L in the ethanol phase, whereas Albe et al. obtained values of 0.76 g/L (1.5 mM) and Theobald et al. 1.06 g/L (2.1 mM) in the cytoplasm. For NAD our values where 1.3 g/L in the glucose phase and 0.55 g/L in the ethanol phase, and Albe obtained 0.71 g/L (1.3 mM) and Theobald 0.71 g/L (1.07 mM) in the cytoplasm. For citrate our values where 0.11 g/L on glucose and 0.07 on ethanol, whereas for Albe it was 0.13 g/L (0.7 mM). Clearly, our values are within the same order of magnitude as those obtained by Albe and Theobald.

Figures 4 and 5 show the qualitative behavior of the model during exponential growth on glucose and during exponential growth on ethanol without glucose, respectively. All fluxes followed the behavior shown by the MFA obtained from experimental results both when cells were growing on glucose or ethanol. Tables V and VI show how well the fluxes, computed with the rate constants determined, shown in Table IV, and using the model, match the fluxes obtained from the MFA during the exponential growth on glucose and ethanol, respectively (Fig. 3).

In Figures 4 (glucose) and 5 (ethanol), it can be seen that the fluxes shown when cells are growing on glucose (Fig. 4) and on ethanol (Fig. 5) exhibit the direction expected from the MFA (Fig. 3). Similarly, the values obtained in this work by a somewhat simplified metabolic network using MFA and those obtained using the continuous model were extremely similar in most cases during growth on glucose and ethanol. Very few values show discrepancies (Tables V and VI). The model was able to simulate a fermentation of *S. cerevisiae* during exponential growth on glucose and exponential growth on ethanol. The differences obtained between the fluxes given by the model and the fluxes determined by the MFA do not exceed 25% in 75% of the cases during exponential growth on glucose, and 20% in 90% of the cases during exponential growth on ethanol.

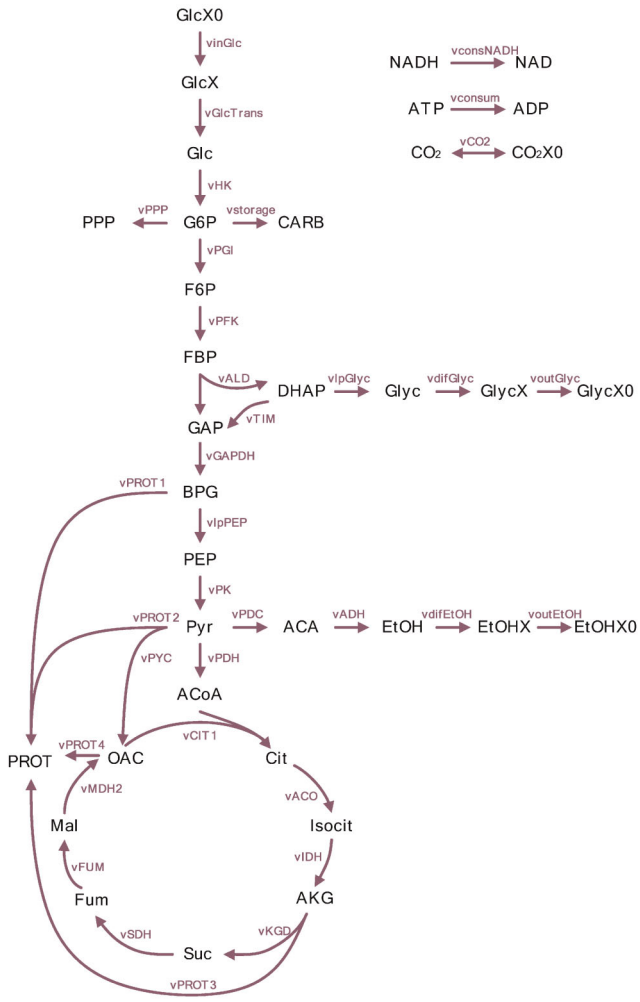

Figure 4. Qualitative behavior of the model during the exponential growth on glucose phase. Arrows correspond to active metabolic fluxes. [Color figure can be seen in the online version of this article, available at wileyonlinelibrary.com]

Figure 6a shows the typical behavior of a glucose-induced enzyme (hexokinase; HK) and a glucose repressed enzyme synthesis (fructose biphosphatase; FBP) during batch fermentation. Figure 6b shows experimental data of the diauxic yeast fermentation for glucose, biomass, and ethanol, and the simulation of the continuous model for the whole batch fermentation which shows an extremely good match between the experimental data and the continuous model with the parameters found. The adjustment of the profiles of biomass, glucose, and ethanol were 95%, 95%, and 79%, respectively. With these results the simulation was considered successful.

The small discrepancies between the fluxes obtained through MFA and those predicted by the differential equations, as well as the good match between the profiles of glucose, biomass, and ethanol, and the simulation show that this simple model, that does not rely on complex kinetic expressions, is able to capture the global behavior of the experimental data. Also, the determination of parameters using a straightforward minimization technique using data

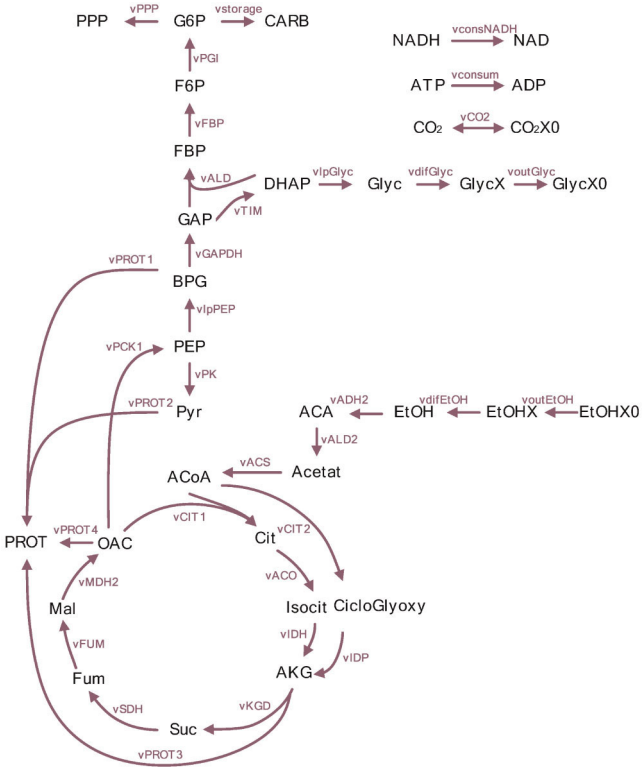

Figure 5. Qualitative behavior of the model during the exponential growth on ethanol phase, without glucose. Arrows correspond to active metabolic fluxes. [Color figure can be seen in the online version of this article, available at wileyonlinelibrary.com]

at only two time points was sufficient to produce a relatively accurate model. Thus, even with a relatively small amount of experimental data (rates and not concentrations) it was possible to estimate the parameters minimizing a simple objective function. It should be realized that the method proposed allows the obtention of reasonable parameters and concentrations in a system with a much larger number of unknowns (120) than equations (72).

The validity of the model has also been tested to be predictive beyond the shift from glucose to ethanol consumption. This was done by testing the effects of deleting the Snf1 and the Mig1 genes. The results have been compared with those reported in the literature (Gancedo, 1998; Klein et al., 1998; Soontorngun et al., 2007). The effect on four of the genes that are directly influenced by Snf1 and Mig1 which are fbp1, adh2, pck1, and idp2 (Table A1) was compared, and in all cases the simulation results obtained, with no glucose repression effect, and thus an important increase in gene expression, were identical to those reported in the literature. The other five genes, also regulated by Snf1 and Mig1 in our model, namely ald2, ald3, acs1, acs2, and cit2 show exactly the same behavior in the simulation.

Previous modeling approaches using continuous modeling and differential equations for the metabolic network mainly correspond to the work carried out by the group of Reuss (Rizzi et al., 1997; Theobald et al., 1997), which did not consider gene regulation of enzymes. Also, in such a continuous model, kinetic parameters of the reactions will change for each different set of conditions such as those when cells are growing on glucose or on ethanol. The only

Table V. Comparison between fluxes given by MFA and the model during exponential growth on glucose and their difference*.

	vinGlc	vGlcTrans	vHK	vPGl	vPFK	vFBP	vALD	vTIM
Model	4.63	4.87	4.82	3.90	3.85	0.00	3.81	1.56
MFA	4.89	4.89	4.89	3.90	3.90	0.00	3.90	2.66
Difference [%]	0.69	0.00	0.05	0.00	0.03	0.00	0.10	22.74
	vGAPDH	vIpPEP	vPK	vPDC	vADH	vADH2	vdifEtOH	voutEtOH
Model	5.34	5.29	5.18	3.44	3.43	0.00	3.29	3.05
MFA	6.56	6.46	5.46	4.27	4.27	0.00	4.27	4.27
Difference [%]	11.34	10.60	12.68	8.07	8.26	0.00	11.25	17.43
	vIpGlyc	vdifGlyc	voutGlyc	vstorage	vALD2	vACS	vPDH	vPYC
Mudel	2.23	2.22	2.22	0.26	0.00	0.00	1.58	0.11
MFA	1.24	1.24	1.24	0.24	0.00	0.00	1.91	0.19
Difference [%]	21.98	21.63	21.63	0.08	0.00	0.00	2.85	1.68
	vCIT1	vACO	vIDH	vKGD	vSDH	vFUM	vMDH2	vPCKl
Mudel	1.57	1.57	1.57	1.51	1.51	1.51	1.51	0.00
MFA	1.91	1.91	1.91	1.80	1.80	1.80	1.80	0.00
Difference [%]	3.03	3.03	3.03	2.34	2.34	2.34	2.34	0.00
	vCIT2	VIDP	vPROT	vPPP	vconsNADH	vconsum	vOUC02	
Model	0.00	0.00	0.39	0.65	1.21	4.34	8.64	
MFA	0.00	0.00	0.71	0.75	2.10	6.35	10.50	
Difference [%]	0.00	0.00	7.21	0.67	18.86	31.81	16.47	

The flux values are given in mmol/g cell h.

*The differences were calculated by the mean square error normalized by the maximum flux value given by the MFA or the model: $E(f_{\mathrm{MFA}}, f_{\mathrm{model}})\% = \frac{\sqrt{(f_{\mathrm{MFA}} - f_{\mathrm{model}})^2}}{\max(f_{\mathrm{MFA}}, f_{\mathrm{model}})} \times 100$.

Table VI. Comparison between fluxes given by MFA and the model during exponential growth on ethanol and their difference*.

	vinGlc	vGlcTrans	vHK	vPGI	vPFK	vFBP	vALD	vTIM
Model	0.00	0.00	0.00	−0.94	0.01	0.87	0.78	−1.15
MFA	0.00	0.00	0.00	−0.65	0.00	0.65	0.65	−0.93
Difference [%]	0.00	0.00	0.00	8.95	0.50	2.78	1.08	2.10
	vGAPDH	vIpPEP	vPK	vPDC	vADH	vADH2	vdifEtOH	voutEtOH
Model	−1.88	−1.94	0.08	0.01	0.03	2.84	−2.62	−2.27
MFA	−1.58	−1.64	0.05	0.00	0.00	3.07	−3.07	−3.07
Difference [%]	2.39	2.32	0.56	0.50	1.30	0.86	3.30	10.42
	vIpGlyc	vdifGlyc	voutGlyc	vstorage	vALD2	vACS	vPDH	vPYC
Mode	0.43	0.44	0.45	0.27	2.92	2.98	0.00	0.00
MFA	0.28	0.28	0.28	0.21	3.07	3.07	0.00	0.00
Difference [%]	2.62	2.91	3.21	0.67	0.37	0.13	0.00	0.00
	vCITl	vACO	vIDH	vKGD	vSDH	vFUM	vMDH2	vPCKl
Model	1.44	1.49	1.58	3.25	3.20	3.27	3.49	2.03
MFA	1.26	1.26	1.26	3.00	3.00	3.00	3.00	1.69
Difference [%]	1.13	1.78	3.24	0.96	0.63	1.11	3.44	2.85
	vCIT2	vIDP	vPROT	vPPP	vconsNADH	vconsum	voutCO2	
Mode	1.60	1.61	0.43	0.69	7.37	6.94	7.52	
MFA	1.82	1.81	0.43	0.44	7.30	7.10	6.39	
Difference [%]	1.33	1.10	0.00	4.53	0.03	0.18	8.49	

The flux values are given in mmol/g cell h.

*The differences were calculated by the mean square error normalized by the maximum flux value given by the MFA or the model: $E(f_{MFA}, f_{model})\% = \frac{\sqrt{(f_{MFA}-f_{model})^2}}{\max(f_{MFA}, f_{model})} \times 100$.

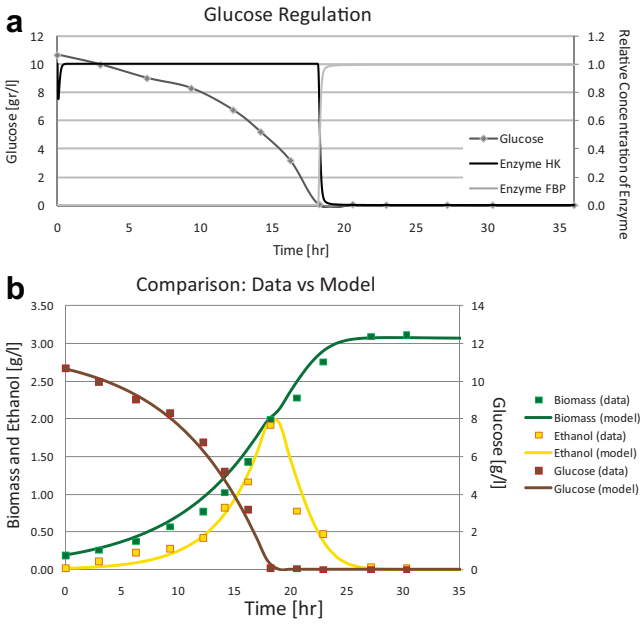

Figure 6. **a**: Enzymatic expression regulated by glucose during the batch fermentation. HK, hexokinase (induced); FBP, fructose bisphosphatase (repressed). **b**: Model simulation. Biomass, glucose, and ethanol profiles during a whole batch fermentation. Profiles given by the model (continuous lines) and its comparison to the experimental data. Experimental results are from González et al. (2003). [Color figure can be seen in the online version of this article, available at wileyonlinelibrary.com]

model that considered the interaction of the genetic regulatory network and its interaction with the metabolic network has been that of Asenjo et al. (2007) which is a discrete model. This study presents a continuous model that includes the presence of genes, the regulation of the synthesis of enzymes by induction, and repression and their influence on the main reactions of the metabolism of *S. cerevisiae*. In addition, in this model, the same set of parameters is used for the different conditions such as growth on glucose or on ethanol.

Conclusions

The continuous mathematical model for the metabolic network, incorporating the information of the genetic regulatory network, allows a quantitative description of the behavior of *S. cerevisiae* during growth on glucose and ethanol. The metabolic network has 39 fluxes, which represent the action of 50 enzymes and 64 genes. The model includes enzyme kinetics, equations that follow both mass-action law and transport as well as inducible, repressible, and constitutive enzymes of the metabolism.

The model was able to simulate a fermentation of *S. cerevisiae* during the exponential growth phase on glucose and the exponential growth phase on ethanol using only one set of kinetic parameters. All fluxes in the continuous model followed the behavior shown by the MFA obtained from experimental results. The differences between the fluxes

given by the model and the fluxes determined by the MFA do not exceed 25% in 75% of the cases during exponential growth on glucose, and 20% in 90% of the cases during exponential growth on ethanol. Furthermore, the adjustment of the profiles of biomass, glucose, and ethanol were 95%, 95%, and 79%, respectively. With these results the simulation was considered successful. In addition, the effect of deleting genes Snf1 and Mig1 in the model showed it to be predictive beyond the shift from glucose to ethanol consumption.

The small discrepancies between the fluxes obtained through MFA and those predicted by the differential equations, as well as the good match between the profiles of glucose, biomass, and ethanol, and our simulation show that this simple model, that does not rely on complex kinetic expressions, is able to capture the global behavior of the experimental data. Also, the determination of parameters using a straightforward minimization technique using data at only two points in time was sufficient to produce a relatively accurate model. Thus, even with a relatively small amount of experimental data (rates and not concentrations) it was possible to estimate the parameters minimizing a simple objective function. Hence, a contribution of this study consists of presenting a convenient way to find in vivo rate parameters to model metabolic and genetic networks under different conditions. It should be realized that the method proposed allows the obtention of reasonable parameters and concentrations in a system with a much larger number of unknowns (120) than equations (72).

Nomenclature

$[A]$	concentration of metabolite A
$[S]$	substrate concentration
$[E]$	enzyme concentration
[mRNA]	mRNA concentration
$[O]$	operator concentration
C	concentration
S	stoichometric matrix
v	rate
K	rate parameter
e	relative enzyme concentration, takes values between 0 and 1.
K_{enz}	enzyme degradation constant
K_{mRNA}	mRNA degradation constant
α	Hill factor
k_r	regulation constant
K_{yield}	yield coefficient
f	flux
t	time
r_i	rate of i reaction
$f_{MFA,i}$	flux i obtained by the MFA
α_w, β_w, γ_w, δ_w, ε_w, φ_w	weight coefficients for minimization
K_{conv}	conversion constant from extracellular to membrane glucose
K_{vinGlc}	rate constant for the glucose flux between the cell membrane and the extracellular space
$K_{voutEtOH}$	rate constant for the ethanol flux between the cell membrane ad the extracellular space

Subscript

max	maximum concentration
t	total concentration
g	during exponential growth on glucose
e	during exponential growth on ethanol
f	rate in forward direction
b	rate in backward direction

Metabolites (Concentrations given in mM)

GlcX0	extracellular glucose
GlycX0	extracellular glycerol
EtOHX0	extracellular ethanol
GlcX	membrane glucose
Glc	intracellular glucose
G6P	glucose-6-phosphate
F6P	fructose-6-phosphate
FBP	fructose bisphosphate
GAP	glyceraldehyde-3-phosphate
DHAP	dihydroxyacetone phosphate
BPG	1,3-biphosphoglycerate
PEP	phosphoenol pyruvate
Pyr	pyruvate
ACA	acetaldehyde
EtOH	intracellular ethanol
EtOHX	ethanol of membrane
Glyc	intracellular glycerol
GlycX	glycerol of membrane
ATP	adenosine triphosphate
ADP	adenosine diphosphate
AMP	adenosine monophosphate
NADH	nicotinamide adenine dinucleotide (reduced form)
NAD	nicotinamide adenine dinucleotide
Acetat	acetate
CoA	coenzyme A
AcoA	acetyl-coenzyme A
OAC	oxaloacetate
Cit	citrate
Isocit	isocitrate
AKG	α-ketoglutarate
Suc	succinate
Fum	fumarate
Mal	malate
CicloGlyoxy	fictitious metabolite to represent the glyoxylate cycle

References

Albe KR, Butler MH, Wright BE. 1990. Cellular concentration of enzymes and their substrates. J Theor Biol 143:163–195.

Alon U. 2007. An introduction to systems biology: Designs principles of biological circuits. USA: Chapman & Hall. p 301.

Asenjo JA, Ramírez P, Rapaport I, Aracena J, Goles E, Andrews BA. 2007. A discrete mathematical model applied to genetic regulation and metabolic networks. J Microbiol Biotechnol 17:496–510.

Bailey JE, Ollis DF. 1986. Biochemical engineering fundamentals. 2nd edn. USA: Mc Graw-Hill. p 984.

Benanti JA, Cheung SK, Brady MC, Toczyski DP. 2007. A proteomic screen reveals SCFGrr1 targets that regulate the glycolytic gluconeogenic switch. Nat Cell Biol 9:1184–1191.

Boube M, Joulia L, Cribbs DL, Bourbon HM. 2002. Evidence for a mediator of RNA polymerase II transcriptional regulation conserved from yeast to man. Cell 110:143–151.

Brusch L, Cuniberti G, Bertau M. 2004. Model evaluation for glycolytic oscillations in yeast biotransformations of xenobiotics. Biophys Chem 109:413–426.

Cox SJ, Levanon SS, Bennett GN, San K. 2005. Genetically constrained metabolic flux analysis. Metab Eng 7:445–456.

Daran-Lapujade P, Jansen ML, Daran JM, van Gulik W, de Winde JH, Pronk JP. 2004. Role of transcriptional regulation in controlling fluxes in central carbon metabolism of *Saccharomyces cerevisiae*. A Chemostat culture study. J Biol Chem 279:9125–9138.

Díaz H, Andrews BA, Hayes A, Castrillo JI, Oliver SG, Asenjo JA. 2009. Global gene expression in recombinant and non-recombinant yeast *Saccharomyces cerevisiae* in three different metabolic states. Biotechnol Adv 27:1092–1117.

Engl HW, Hanke M, Neubauer A. 2000. Regularization of inverse problems (mathematics and its applications). Dordrecht, The Netherlands: Kluwer Academic Publishers.

Famili I, Förster J, Nielsen J, Palsson BO. 2003. *Saccharomyces cerevisiae* phenotypes can be prediBTed by using constraint-based analysis of a genome-scale reconstruBTed metabolic network. Proc Natl Acad Sci USA 100:13134–13139.

Gagneur J, Casari G. 2005. From molecular networks to qualitative cell behavior. Sys Biol FEBS Lett 579:1867–1871.

Gancedo J. 1998. Yeast carbon catabolite repression. Microbiol Mol Biol Rev 62:334–361.

Gombert AK, Moreira dos Santos M, Christensen B, Nielsen J. 2001. Network identification and flux quantification in the central metabolism of *Saccharomyces cerevisiae* under different conditions of glucose repression. J Bacteriol 183:1441–1451.

González R, Andrews BA, Molitor J, Asenjo JA. 2003. Metabolic analysis of the synthesis of high levels of intracellular human SOD in *Saccharomyces cerevisiae* rhSOD 2060 411 SGA 122. Biotechnol Bioeng 82:152–169.

Hatzimanikatis V. 2010. Course: Systems biology. Santiago, Chile: Institute for Cell Dynamics and Biotechnology, University of Chile.

Hynne F, Danø S, Sørensen PG. 2001. Full-scale model of glycolysis in *Saccharomyces cerevisiae*. Biophys Chem 94:121–163.

Jacob F, Monod J. 1961. Genetic regulatory mechanism in the synthesis of proteins. J Mol Biol 3:318–356.

Kaushik K, Condo S, Venkatasubramanian K. 1979. Modeling of inducible enzyme biosynthesis in microbial cells. Ann N Y Acad Sci 326:57–71.

Klein CJL, Olsson L, Nielsen J. 1998. Glucose control in *Saccharomyces cerevisiae*: The role of M/G7 in metabolic functions. Microbiology 144:13–24.

Lagunas R, Gancedo C. 1983. Role of phosphate in the regulation of the Pasteur effect inSaccharomyces cerevisiae. Eur J Biochem 137:479–483.

Müller S, Bole E, May M, Zimmermann F. 1995. Different internal metabolites trigger the inductions of glycolytic gene expression in *Saccharomyces cerevisiae*. J Bacteriol 177:4517–4519.

Özcan S, Dover J, Rosenwald AG, Wölfl S, Johnston M. 1996. Two glucose transporters in *Saccharomyces cerevisiae* are glucose sensors that generate a signal for induction of gene expression. Proc Natl Acad Sci USA 93:12428–12432.

Özcan S, Dover J, Johnston M. 1998. Glucose sensing and signaling by two glucose receptors in the yeast *Saccharomyces cerevisiae*. EMBO J 17:2566–2573.

Rizzi M, Baltes M, Theobald U, Reuss M. 1997. *In vivo* analysis of metabolic dynamics in *Saccharomyces cerevisiae*: II. Mathematical model. Biotechnol Bioeng 55:592–608.

Rolland F, Winderickx J, Thevelein JM. 2002. Glucose-sensing and -signalling mechanism in yeast. FEMS Yeast Res 2:183–201.

Santangelo GM. 2006. Glucose signaling in *Saccharomyces cerevisiae*. Microbiol Mol Biol Rev 70:253–282.

Schüller HJ. 2003. Transcriptional control of nonfermentative metabolism in the yeast *Saccharomyces cerevisiae*. Curr Genet 43:139–160.

Soontorngun N, Larochelle M, Drouin S, Robert F, Turcotte B. 2007. Regulation of gluconeogenesis in *Saccharomyces cerevisiae* is mediated by activator and repressor functions of Rds2. Mol Cell Biol 27:7895–7905.

Teusink B, Passarge J, Reijenga CA, Esgalhado E, van der Weijden CC, Schepper M, Walsh MC, Bakker BM, van Dam K, Westerhoff HV, Snoep JL. 2000. Can yeast glycolysis be understood in terms of in vitro kinetics of the constituent enzymes? Testing biochemistry. Eur J Biochem 267:5313–5329.

Theobald U, Mailinger W, Baltes M, Rizzi M, Reuss M. 1997. In vivo analysis of metabolic dynamics in *Saccharomyces cerevisiae*: I. Experimental observations. Biotechnol Bioeng 55:305–316.

Wang L, Hatzimanikatis V. 2006. Metabolic engineering under uncertainty—II: Analysis of yeast metabolism. Metab Eng 8:142–159.

Wiechert W. 2002. Modeling and simulation: Tools for metabolic engineering. J Biotechnol 94:37–63.

Yagil G, Yagil E. 1971. On the relation between effect or concentration and the rate of induced enzyme synthesis. Biophys J 11:11–27.

Zhang N, Wu J, Oliver SG. 2009. Gis1 is required for transcriptional reprogramming of carbon metabolism and the stress response during transition into stationary phase in yeast. Microbiology 155:1690–1698.

Appendix 1

Table A1.

Table A1. Genes and enzymes that participate in each reaction of the network.

Rate	Enzyme	Gene
vinGlc	—	—
vGlcTrans	Hexose transporter	hxt1
	Hexose transporter	hxt2
	Hexose transporter	hxt3
	Hexose transporter	hxt4
	Hexose transporter	hxt5
	Hexose transporter	hxt6
	Hexose transporter	hxt7
vHK	Hexokinase A	hxk1
	Hexokinase B	hxk2
	Glucokinase	glk1
vPGI	Phosphoglucoisomerase	pgi1
vPFK	Phosphofructokinase (dimer)	pfk1, pfk2
vFBP	Fructose-1,6-bisphosphatase	fbp1
vALD	Aldolase	fba1
vTIM	Triose-phosphate isomerase	tpi1
vGAPDH	Glyceraldehyde-3-phosphate dehydrogenase (tetramer)	tdh1,tdh2,tdh3
vlpPEP	Enolase (dimer)	eno1, eno2
	3-Phosphoglycerate kinase	pgk1
	Glycerate phosphomutase	gpm1
vPK	Pyruvate kinase	pyk1
	Pyruvate kinase	pyk2
vPDC	Pyruvate decarboxylase	pdc1
	Pyruvate decarboxylase	pdc5
	Pyruvate decarboxylase	pdc5
vADH	Alcohol dehydrogenase	adh1
	Alcohol dehydrogenase	adh3
	Alcohol dehydrogenase	adh4
vADH2	Alcohol dehydrogenase II	adh2
vdifEtOH	—	—
voutEtOH	—	—
vlpGlyc	Glycero l-3-phosphate dehydrogenase	gpd1
	Glycerol-3-phosphate dehydrogenase	gpd2
	DL-glycerol-3-phosphatase	gpp1
	DL-glycerol-3-phosphatase	hor2
vdifGlyc	—	—
voutGlyc	—	—
vstorage	[a]	[a]
vALD2	Aldehyde dehydrogenase	ald2
	Aldehyde dehydrogenase	ald3
vACS	Acetyl CoAsynthetase	acs1
	Acetyl CoAsynthetase	acs2
vPDH	Pyruvate dehydrogenase (complex)	pda1, pda2, pdb1, lpd1, pdx1
vPYC	Pyruvate carboxylase	pyc1
	Pyruvate carboxylase	pyc2
vCIT1	Citrate synthetase	cit1
vACO	Aconitase	aco1
vIDH	Isocitrate dehydrogenase (complex)	idh1, idh2
vKGD	Alpha-ketoglutarate dehydrogenase (complex)	Kgd1, kgd2
	Ligase of succinyl-CoA	lsc1, lsc2
vSDH	Succinate dehydrogenase (complex)	sdh1,sdh2, sdh3,sdh4
vFUM	Fumarase (fumarate hydrolase)	fuml
vMDH2	Malate dehydrogenase (cytosolic)	mdh2
vPCK1	Phosphoenolpyruvate carboxykinase	pck1
vCIT2	Citrate synthase	cit2
vIDP	Isocitrate dehydrogenase, NADP-specific	idp2
vPROT	[a]	[a]
vPPP	[a]	[a]
vconsNADH	[a]	[a]
vconsum	[a]	[a]
voutCO2	[a]	[a]

— Indicates rate without enzyme (or gene).

[a]Rate that has been simplified because it contemplates a great number of enzymes and genes.